TENCON 2023 - 2023 IEEE Region 10 Conference (TENCON)
31 Oct - 3 Nov 2023. Chiang Mai, Thailand

Variable Bandpass Filters with Full-Band Tunability and Absolutely Guaranteed Stability

Tian-Bo Deng
Department of Information Science
Faculty of Science, Toho University, Japan
deng@is.sci.toho-u.ac.jp

***Abstract*—Variable digital filters are reconfigurable signal processing systems that possess tunable frequency responses. Therefore, a variable digital filter can carry out real-time online tuning during filtering operations. To produce a new response in a timely manner, the transfer-function's coefficients of a variable filter must be the functions of the parameter that is adopted for tuning the filter's response. In this way, the coefficients are changeable. This paper considers designing a variable bandpass filter with a full-band tunable center-frequency (CF). Since the CF can be changed by using the CF parameter, one can represent the filter coefficients as the functions of the CF parameter. Another stiff problem that needs to be carefully solved is the stability issue. The reason is that updating the filter coefficients during online tuning may incur instability. This paper deals with this stability issue by locating the filter's coefficients inside the stability triangle through parameter transformations. To this end, we transform the denominator coefficients into other unconstrained parameters that can take any values without causing instability. After the transformations, a nonlinear optimizer can be used for optimizing the new parameters. A set of fixed-coefficient bandpass filters with full-band tunable CFs are designed for illustrating the achieved stability guarantee together with the achieved considerably accurate approximations.**

I. Introduction

Digital filter is the most fundamental digital system that is considerably useful in a great number of data processing fields, including processing various measurement signals and communication data. Digital filter's usefulness lies in the frequency selectivity. That is, digital filters are able to select important frequency components and cut off unimportant ones. In digital communications, digital filters are utilized for limiting frequency bands. Furthermore, many filter applications need a digital filter that has tunable frequency-domain characteristics [1]-[15]. Various frequency responses can be instantly attained by employing such variable digital filters. Although nonrecursive variable filters are undoubtedly stable, the recursive ones have the stability problem. Thus, the stability problem must be treated carefully.

This paper considers designing a stable variable bandpass filter with adjustable passband center-frequency (CF). The bandpass filter has a variable center-frequency (VCF), and the CF can be tuned in the full frequency band (full-band). As compared to the one in [5], this novel specification has a wider tuning range. Such a VCF bandpass filter is a variable signal processing system with variable system coefficients. For a given VCF bandpass design specification, the target is to determine the optimal transfer function for approximating the ideal VCF bandpass response as accurately as possible. This paper uses the p-norm error criterion to measure the filter's deviations. In addition, the passband CF is specified by using the CF parameter. To get a VCF bandpass filter, every filter coefficient is realized as a function of the CF parameter. To get those functions, a two-step procedure is used in the design process. The first step discretizing a given VCF bandpass specification, and then approximates the discretized ones separately. After producing all those bandpass filters, the second step fits polynomials to the attained filter-coefficient values. This step yields various fitting polynomials.

The difficult issue in designing such a filter lies in the stability guarantee. This is done by positioning all the denominator coefficients of the VCF bandpass filter within the stability triangle. To this end, parameter transformations on the denominator coefficients are performed. To confirm the achieved stability, a variety of fixed-coefficient bandpass filters with different CFs are designed and tested. Computer simulation results are also given for demonstrating the achieved stability as well as the approximation accuracy.

II. Full-Band VCF Specification

We consider approximating the bandpass VCF specification

$$\mathcal{S}(\omega,\lambda)=\begin{cases}0, & \omega\in[0,\omega_{\mathrm{s1}}]\\ \dfrac{\omega-\omega_{\mathrm{s1}}}{\omega_{\mathrm{p1}}-\omega_{\mathrm{s1}}}, & \omega\in[\omega_{\mathrm{s1}},\omega_{\mathrm{p1}}]\\ 1, & \omega\in[\omega_{\mathrm{p1}},\omega_{\mathrm{p2}}]\\ \dfrac{\omega_{\mathrm{s2}}-\omega}{\omega_{\mathrm{s2}}-\omega_{\mathrm{p2}}}, & \omega\in[\omega_{\mathrm{p2}},\omega_{\mathrm{s2}}]\\ 0, & \omega\in[\omega_{\mathrm{s2}},\pi]\end{cases} \tag{1}$$

where $\omega\in[0,\pi]$ is used to denote the normalized frequency. The CF of the passband $[\omega_{\mathrm{p1}},\omega_{\mathrm{p2}}]$ is tuned by the parameter

$$\lambda\in[0.3\pi,0.7\pi] \tag{2}$$

and the two passband edge frequencies are defined by

$$(\omega_{\mathrm{p1}},\omega_{\mathrm{p2}})=(\lambda-0.2\pi,\lambda+0.2\pi). \tag{3}$$

Moreover, the two stopband edge frequencies are

$$\begin{aligned}\omega_{\mathrm{s1}}&=\omega_{\mathrm{p1}}-0.10\pi=\lambda-0.3\pi\\ \omega_{\mathrm{s2}}&=\omega_{\mathrm{p2}}+0.10\pi=\lambda+0.3\pi.\end{aligned} \tag{4}$$

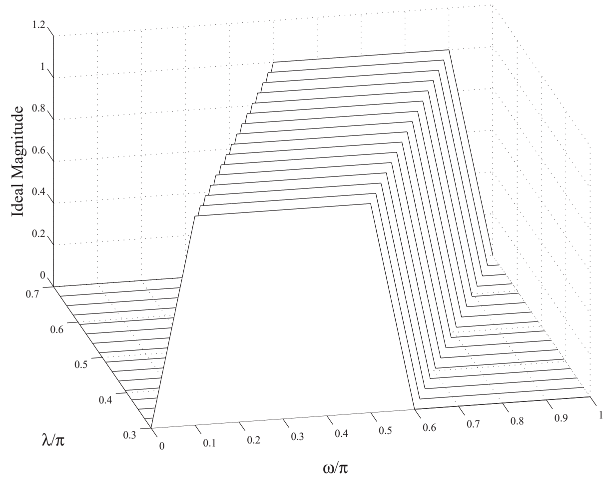

Fig. 1. Desired full-band VCF responses.

The parameter λ is called CF parameter, which is used for tuning the passband CF. Clearly, the width of the passband $\omega \in [\omega_{\rm p1}, \omega_{\rm p2}]$ remains unchanged (0.4π), and the two transition bands $\omega \in [\omega_{\rm s1}, \omega_{\rm p1}]$ and $\omega \in [\omega_{\rm p2}, \omega_{\rm s2}]$ have a fixed width (0.10π). One can conclude from the above parameter settings that the passband CF varies in the full frequency band.

Here, we use the coefficient-parameterized transfer function

$$T(z,\lambda) = \frac{\displaystyle\sum_{i=0}^{I_1} d_i(\lambda) z^{-i}}{\displaystyle\prod_{i=1}^{I_2} \left(1 + c_{i,1}(\lambda) z^{-1} + c_{i,2}(\lambda) z^{-2}\right)} \tag{5}$$

whose amplitude response fits $S(\omega,\lambda)$ in (1). As λ varies, the passband CF of $S(\omega,\lambda)$ in (1) continuously varies. To approximate $S(\omega,\lambda)$, we first equally sample the interval in (2) by using the same stepsize $0.4\pi/(L-1)$, $L = 16$. This produces L equally-spaced samples λ_l. That is,

$$\lambda \in [0.3\pi, 0.7\pi] \longrightarrow \lambda_1, \lambda_2, \cdots, \lambda_L.$$

The corresponding discretized specifications are

$$S(\omega,\lambda_1), S(\omega,\lambda_2), \cdots, S(\omega,\lambda_L). \tag{6}$$

Those specifications $S(\omega,\lambda_l)$ are given in Fig. 1, which have different passband CFs, but the same passband width (0.4π).

III. Two-Step Design Method

The design tries to determine the optimum coefficients

$$d_i(\lambda), c_{i,1}(\lambda), c_{i,2}(\lambda)$$

as the functions of λ. This is achieved by executing the following 2 separate steps.

A. *Step-1: Designing Constant Bandpass Filters $T_l(z)$*

This step approximates each bandpass VCF specification $S(\omega,\lambda_l)$ in (6) by using a constant bandpass filter

$$T_l(z) = \frac{\displaystyle\sum_{i=0}^{I_1} d_i z^{-i}}{\displaystyle\prod_{i=1}^{I_2} [1 + c_{i,1} z^{-1} + c_{i,2} z^{-2}]}. \tag{7}$$

Specifically, the transfer functions are individually related to the specifications $S(\omega,\lambda_l)$ as

$$\begin{aligned} T_1(z) &\Longleftrightarrow S(\omega,\lambda_1) \\ T_2(z) &\Longleftrightarrow S(\omega,\lambda_2) \\ &\vdots \\ T_L(z) &\Longleftrightarrow S(\omega,\lambda_L). \end{aligned} \tag{8}$$

Each of the above approximations minimizes the p-norm error (deviation), leading to a nonlinear programming problem. Before proceeding with the nonlinear minimization, a critical issue involving the stability needs to be carefully addressed. In other words, the resulting filter $T_l(z)$ in (7) may be unstable unless the coefficients $c_{i,1}, c_{i,2}$ in its denominator meet the stability condition

$$\begin{cases} |c_{i,1}| < 1 + c_{i,2} \\ |c_{i,2}| < 1. \end{cases} \tag{9}$$

To ensure the stability of the filter $T_l(z)$, it is necessary to impose the stability condition in (9) on the above-mentioned minimization. Indeed, the two inequalities in (9) specify a stable region known as stability triangle. If all points $(c_{i,1}, c_{i,2})$ are forced to move within the triangle, the filter $T_l(z)$ is stable. Evidently, only the coefficients $\{c_{i,1}, c_{i,2}\}$ in the denominator of $T_l(z)$ influence the stability. Therefore, one should not directly optimize $\{c_{i,1}, c_{i,2}\}$. This is because the direct optimization may produce an unstable filter $T_l(z)$.

This paper tackles this issue by transforming $\{c_{i,1}, c_{i,2}\}$ into the functions of another set of unknowns $\{x_{i,1}, x_{i,2}\}$ as also shwn in [5]. The transformations utilize a function $g(x)$ to transform $\{c_{i,1}, c_{i,2}\}$ into

$$\begin{cases} c_{i,1} = \beta \cdot g(x_{i,1})(1 + c_{i,2}) \\ c_{i,2} = \beta \cdot g(x_{i,2}). \end{cases} \tag{10}$$

In the above transformations, a constant $0 < \beta < 1$ is fixed, and $g(x)$ features

$$|g(x)| \le 1. \tag{11}$$

The above transformations guarantee that the stability condition (9) is met for any $\{x_{i,1}, x_{i,2}\}$. The transformations mean that an arbitrary point $(x_{i,1}, x_{i,2})$ in the $x_{i,1}$-$x_{i,2}$ plane can be mapped to the point $(c_{i,1}, c_{i,2})$ in the $c_{i,1}$-$c_{i,2}$ plane, and the point $(c_{i,1}, c_{i,2})$ definitely falls into the inside of the stability triangle. Hence, the design methodology is to optimize the new unknowns $x_{i,1}, x_{i,2}$ based on the transformations in (10)

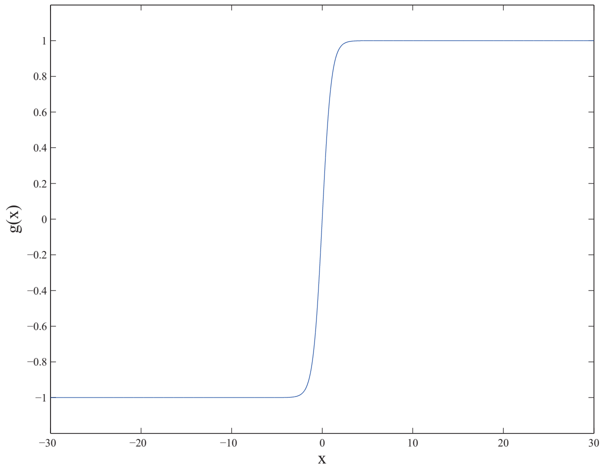

Fig. 2. Function employed for transformations.

rather than directly optimize $\{c_{i,1}, c_{i,2}\}$. This trick leads to a stable recursive bandpass filter $T_l(z)$. This paper employs the function

$$g(x) = \tanh(x)$$

as shown in Fig. 2. This function meets $|g(x)| \leq 1$, and it is also used in [5].

Based on the transformations in (10), we design $T_l(z)$ one by one, $l = 1, 2, \cdots, L$. The optimum values of $\{d_i, x_{i,1}, x_{i,2}\}$ are determined such that the p-norm of the amplitude deviations is minimized. For example, designing $T_1(z)$ for approximating $S(\omega, \lambda_1)$ implies that $\{d_i, x_{i,1}, x_{i,2}\}$ are optimized by minimizing the p-norm deviation

$$\delta_p = \left[\sum_{k=1}^{K} W(\omega_k)|\delta(\omega_k)|^p\right]^{1/p} \tag{12}$$

where ω_k ($k = 1, 2, \cdots, K$) are discretized frequencies in $[0, \pi]$, $\delta(\omega_k)$ is the approximation error at frequency ω_k, i.e.,

$$\delta(\omega_k) = S(\omega_k, \lambda_1) - T_1(\omega_k)$$

and $T_1(\omega_k)$ is the amplitude response of $T_1(z)$.

B. Step-2: Getting VCF Bandpass Filter

After $T_l(z)$, $l = 1, 2, \cdots, L$, are attained, the optimized values of $\{d_i, x_{i,1}, x_{i,2}\}$ are available. That is, each $T_l(z)$ corresponds to its coefficient values as

$$\begin{aligned} T_1(z) &\longleftrightarrow \{d_i, x_{i,1}, x_{i,2}\} \\ T_2(z) &\longleftrightarrow \{d_i, x_{i,1}, x_{i,2}\} \\ &\vdots \\ T_L(z) &\longleftrightarrow \{d_i, x_{i,1}, x_{i,2}\}. \end{aligned} \tag{13}$$

The next step is to fit each coefficient values, say d_1, by using a polynomial in λ. This fitting operations produce all the polynomials

$$d_i(\lambda), x_{i,1}(\lambda), x_{i,2}(\lambda).$$

As a result, the final VCF bandpass filter $T(z, \lambda)$ in (5) can be attained by utilizing the changeable coefficients

$$d_i(\lambda), c_{i,1}(\lambda), c_{i,2}(\lambda)$$

where $c_{i,1}(\lambda)$ and $c_{i,2}(\lambda)$ are generated from $x_{i,1}(\lambda)$ and $x_{i,2}(\lambda)$ by employing the transformations

$$\begin{cases} c_{i,2}(\lambda) = \beta \cdot g(x_{i,2}(\lambda)) \\ c_{i,1}(\lambda) = \beta \cdot g(x_{i,1}(\lambda))[1 + c_{i,2}(\lambda)]. \end{cases} \tag{14}$$

IV. Computer Simulations

The ideal VCF bandpass magnitude response in (1) is approximated using the parameter settings

$$\begin{aligned} (I_1, I_2) &= (8, 4) \\ (K, L) &= (1001, 16) \\ (p, \beta) &= (100, 0.99). \end{aligned}$$

The weighting function in (12) is

$$W(\omega_k) = \begin{cases} 1, & \omega_k \in [0, \omega_{\mathrm{s1}}] \cup [\omega_{\mathrm{p1}}, \omega_{\mathrm{p2}}] \cup [\omega_{\mathrm{s2}}, \pi] \\ 0.2, & \text{transition bands.} \end{cases} \tag{15}$$

The computer simulations employ a nonlinear programming to minimize the p-norm error in (12). Starting at zero initial coefficient values for the minimization, we get the positions of $(c_{i,1}, c_{i,2})$ along with the stability triangles illustrated in Fig. 3 for $T_l(z)$, $l = 1, 2, \cdots, L$. Fig. 3 illustrates that all the points $(c_{i,1}, c_{i,2})$ are forced to be located within the triangles. This is attributed to the transformations adopted. Therefore, Fig. 3 confirms that the stability has been achieved. Furthermore, Fig. 4 plots the positions of all the poles for $T_l(z)$, $l = 1, 2, \cdots, L$. Clearly, all the poles are positioned within the unit circles, which is also consistent with the achieved stability. Fig. 5 depicts the amplitude responses of the obtained $T_l(z)$, $l = 1, 2, \cdots, L$.

The approximation accuracy of each $T_l(z)$ is assessed by computing the errors

$$\begin{aligned} \delta_p &= \left[\sum_{k=1}^{K} W(\omega_k)|\delta(\omega_k)|^p\right]^{1/p} \\ \delta_{\max} &= \max\{W(\omega_k)|\delta(\omega_k)|\} \\ \delta_2 &= \sqrt{\frac{\sum_{k=1}^{K}|\delta(\omega_k)|^2}{\sum_{k=1}^{K}|S(\omega_k, \lambda_l)|^2}} \times 100\% \end{aligned}$$

where ω_k are frequency samples in $[0, \pi]$, and

$$\delta(\omega_k) = S(\omega_k, \lambda_l) - T_l(\omega_k)$$

represents the error at frequency ω_k, $T_l(\omega_k)$ is the gain response of $T_l(z)$. The mean values are

$$\overline{\delta}_p = 0.020439, \quad \overline{\delta}_{\max} = 0.020088, \quad \overline{\delta}_2 = 2.123088\%.$$

979-8-3503-0219-6/23/$31.00 ©2023 IEEE

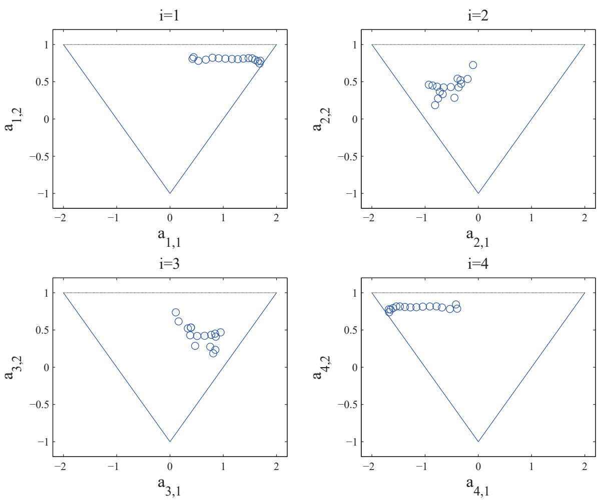

Fig. 3. Checking positions of $(c_{i,1}, c_{i,2})$.

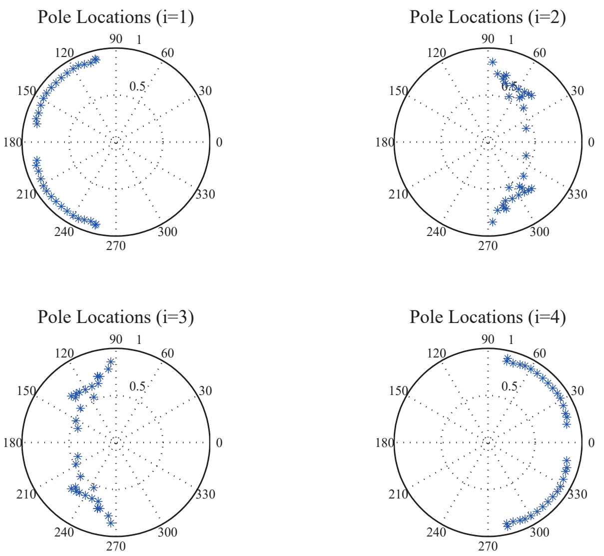

Fig. 4. Checking positions of poles.

V. Conclusion

A two-step design method incorporating transformations has been detailed for achieving stable bandpass filters with full-band tunable CFs. To ensure the stability of the resultant bandpass filters from the nonlinear minimization, the original denominator-coefficient pairs are first converted to another set of new unknowns. Then, the nonlinear minimization is executed for optimizing the coefficients. This ensures that the denominator-coefficient points are definitely positioned within the stability triangle, and thus the resulting bandpass filters are stable. The coefficients of a VCF bandpass filter can be obtained as the functions of the CF parameter λ through fitting the coefficient values of the bandpass filters $T_l(z)$.

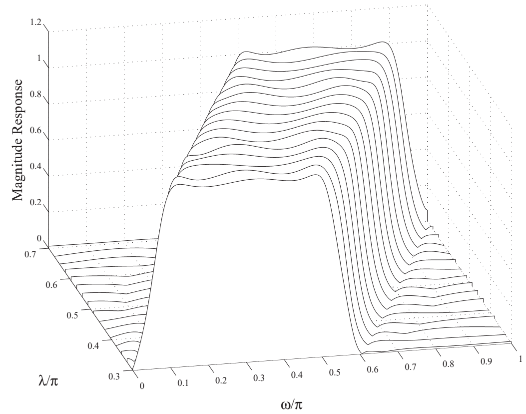

Fig. 5. Checking the actual magnitudes of $T_l(z)$.

References

[1] R. Zarour and M. M. Fahmy, "A design technique for variable digital filters," *IEEE Trans. Circuits Syst.*, vol. 36, no. 11, pp. 1473-1478, Nov. 1989.

[2] T.-B. Deng, "Design of recursive 1-D variable filters with guaranteed stability," *IEEE Trans. Circuits Syst. II, Analog Digit. Signal Process.*, vol. 44, no. 9, pp. 689-695, Sep. 1997.

[3] T.-B. Deng, "Design of recursive variable-digital-filters with theoretically-guaranteed stability," *International Journal of Electronics*, vol. 103, no. 12, pp. 2013-2028, Dec. 2016.

[4] T.-B. Deng, "The Lp-norm-minimization design of stable variable-bandwidth digital filters," *Journal of Circuits, Systems, and Computers*, vol. 27, no. 7 (1850102), pp. 1-18, Jun. 2018.

[5] T.-B. Deng, "Design and stability guarantee of variable center-frequency bandpass filters," *Proc. IEEE JCSSE 2023*, pp. 1-6, Phitsanulok, Thailand, Jun. 28-Jul. 1, 2023.

[6] P. Sutthikarn, S. Chivapreecha, A. Trirat, and T. Jongsataporn, "A simple tunable biquadratic digital bandpass filter design for spectrum sensing in cognitive radio," *Proc. IEEE ECTI-CON 2020*, pp. 71-75, Jun. 24-27, 2020, Phuket, Thailand.

[7] T.-B. Deng, "Discretization-free design of variable fractional-delay FIR digital filters," *IEEE Trans. Circuits Syst. II, Analog Digit. Signal Process.*, vol. 48, no. 6, pp. 637-644, Jun. 2001.

[8] T.-B. Deng, "Design and parallel implementation of FIR digital filters with simultaneously variable magnitude and non-integer phase-delay responses," *IEEE Trans. Circuits Syst. II: Analog and Digital Signal Processing*, vol. 50, pp. 243-250, May 2003.

[9] T.-B. Deng, "Closed-form design and efficient implementation of variable digital filters with simultaneously tunable magnitude and fractional-delay," *IEEE Trans. Signal Processing*, vol. 52, pp. 1668-1681, Jun. 2004.

[10] T.-B. Deng and Y. Nakagawa, "SVD-based design and new structures for variable fractional-delay digital filters," *IEEE Trans. Signal Processing*, vol. 52, pp. 2513-2527, Sep. 2004.

[11] T.-B. Deng, Y. Lian, "Weighted-least-squares design of variable fractional-delay FIR filters using coefficient symmetry," *IEEE Trans. Signal Processing*, vol. 54, no. 8, pp. 3023-3038, Aug. 2006.

[12] T.-B. Deng, "Minimax design of low-complexity even-order variable fractional-delay filters using second-order cone programming," *IEEE Trans. Circuits Syst. II: Express Briefs*, vol. 58, no. 10, pp. 692-696, Oct. 2011.

[13] T.-B. Deng, "Decoupling minimax design of low-complexity variable fractional-delay FIR digital filters," *IEEE Trans. Circuits Syst. I: Regular Papers*, vol. 58, no. 10, pp. 2398-2408, Oct. 2011.

[14] T.-B. Deng, S. Chivapreecha, and K. Dejhan, "Bi-minimax design of even-order variable fractional-delay FIR digital filters," *IEEE Trans. Circuits Syst. I: Regular Papers*, vol. 59, no. 8, pp. 1766-1774, Aug. 2012.

[15] P. Soontornwong, T.-B. Deng, and S. Chivapreecha, "Low-complexity and high-modularity structure for implementing transient-free Pascal-delay filter," *IEEE Trans. Signal Processing*, vol. 65, no. 23, pp. 6233-6243, Dec. 2017.